Published in final edited form as:
Virology. 2013 June 5; 440(2): 190–203. doi:10.1016/j.virol.2013.02.021.

HIV-1 Vpu affects the anterograde transport and the glycosylation pattern of NTB-A

Sebastian Bolduan[1], **Philipp Hubel**[1], **Tatjana Reif**[1], **Veronika Lodermeyer**[1], **Kristin Höhne**[4], **Joëlle V. Fritz**[3], **Daniel Sauter**[2], **Frank Kirchhoff**[2], **Oliver T. Fackler**[3], **Michael Schindler**[4], and **Ulrich Schubert**[1]

[1]Institute of Virology, University of Erlangen-Nuremberg, Germany

[2]Institute of Molecular Virology, Ulm University Medical Center, Germany

[3]Department of Infectious Diseases, Virology, University Hospital Heidelberg, Germany

[4]Institute of Virology, Helmholtz Zentrum Munich, Germany

Abstract

HIV-1 Vpu induces downregulation of cell surface NTB-A to evade lysis of HIV-1 infected cells by NK cells. Here we show that Vpu affects the anterograde transport and the glycosylation pattern of NTB-A by a mechanism that is distinct from the Vpu induced downregulation of CD4 and tetherin. In the presence of Vpu, only the high mannose form of NTB-A was detectable, suggesting that Vpu prevented the formation of the mature form of NTB-A. This phenomenon is associated with the ability of Vpu to downregulate cell surface NTB-A by retention of NTB-A within the Golgi-compartment. Furthermore, the Vpu-mediated effect on NTB-A glycosylation is highly conserved among Vpu proteins derived from HIV-1 and SIV and corresponds to the level of downregulation of NTB-A. Together, these results suggest that the reduction of NTB-A from the cell surface is associated with the Vpu-mediated effect on the glycosylation pattern of newly synthesized NTB-A molecules.

Keywords

Vpu; NTB-A; SLAMF6; HIV-1; SIV; *pulse-chase*; N-linked glycosylation; tetherin

Introduction

The human immunodeficiency virus type 1 (HIV-1) accessory protein Vpu is a 15–20 kDa oligomeric type 1 integral membrane phosphoprotein (Cohen et al., 1988; Maldarelli et al., 1993; Strebel, Klimkait, and Martin, 1988), which is encoded exclusively by HIV-1 and related simian immunodeficiency viruses (SIVs), but not by the majority of SIVs and HIV-2. Vpu induces the degradation of newly synthesized CD4, by retaining it in the endoplasmic reticulum (ER) (Magadan et al., 2010) and thereby targeting CD4 to the ER-associated protein degradation (ERAD)-pathway (Binette et al., 2007; Magadan et al., 2010; Schubert

Corresponding author: Ulrich Schubert, Ph.D., Professor of Virology, Institute for Clinical and Molecular Virology, University of Erlangen-Nürnberg, Schlossgarten 4, 91054 Erlangen, Germany, Phone office 49-9131-8526478, Phone Lab 49-9131-8522103, Fax 49-9131-8526182, Ulrich.Schubert@viro.med.uni-erlangen.de.

et al., 1998; Willey et al., 1992). The cytoplasmic domain of Vpu contains a pair of highly conserved serine residues, which are constitutively phosphorylated by the casein kinase 2 (CK-2) (Schubert et al., 1994). This phosphorylation allows binding of the β-transducin repeat containing protein (β-TrCP), a component of the Skp1-Cullin-F-box (SCF) E3 ubiquitin ligase complex (Butticaz et al., 2007; Margottin et al., 1998), which induces polyubiquitination of the cytoplasmic domain of CD4 (Magadan et al., 2010). Consequently, CD4 is retranslocated into the cytosol and degraded by the 26S proteasome (Binette et al., 2007; Magadan et al., 2010; Schubert et al., 1998). Furthermore, it was shown that Vpu supports HIV-1 virion release by counteracting the cellular restriction factor tetherin (also known as CD317, BST-2 or HM1.24) (Neil, Zang, and Bieniasz, 2008; Van Damme et al., 2008). The ability of Vpu to enhance virion release directly correlates with its ability to downregulate cell surface tetherin. The transmembrane (TM) domain of Vpu is essential for interaction with tetherin and consequently for the downregulation of tetherin from the cell surface (Banning et al., 2010; Bolduan et al., 2011; Dube et al., 2010; Iwabu et al., 2009; Rong et al., 2009). This physical interaction likely enables Vpu to trap newly synthesized and recycling tetherin molecules at the level of the trans-Golgi network (TGN) in order to reduce cell surface exposure of the restriction factor (Dube et al., 2010; Schmidt et al., 2011).

In addition to its role in tetherin antagonism and CD4 degradation, the TM domain of Vpu was found to form a non-selective, voltage gated ion channel in planar lipid bilayers (Ewart et al., 1996; Schubert et al., 1996b), which was later continued for the full length molecule (Marassi et al., 1999). Randomization of the TM domain prevents Vpu's ion channel formation and impairs its ability to regulate virion release (Schubert et al., 1996a), indicating a correlation between the ion channel activity of Vpu and its augmentation of virus release. However, it was shown that ion channel activity of Vpu is dispensable for counteraction of tetherin (Bolduan et al., 2011; Kuhl et al., 2011; Skasko et al., 2011).

Recently, it has been described that Vpu induces downregulation of the coactivating NK cell receptor NK, T-cell, B-cell antigen (NTB-A) (also termed CD352 or SLAMF6), as well as the activating NK cell receptor PVR/CD155, from the cell surface to evade lysis of HIV-1 infected cells by NK cells (Matusali et al., 2012; Shah et al., 2010). However, the molecular mechanism of these Vpu induced downregulations, particularly of NTB-A, has not been elucidated so far.

NK cell-mediated degranulation requires two signals from activating and coactivating receptors (Sowrirajan and Barker, 2011). The coactivating NK cell receptor NTB-A, which facilitates NK cell-mediated cytotoxicity (Bottino et al., 2001; Flaig, Stark, and Watzl, 2004), is a type I transmembrane glycoprotein and a member of the signaling lymphocytic activation molecule (SLAM) receptor family (Bottino et al., 2001). It has been suggested that the Vpu induced downregulation of cell surface NTB-A is mechanistically distinct from the downmodulation of CD4 and tetherin (Shah et al., 2010). Furthermore, Vpu does neither increase internalization rates nor alters the steady state protein level of NTB-A (Shah et al., 2010).

Here we demonstrate that in the presence of Vpu only the high mannose form of NTB-A is detectable, suggesting that Vpu prevents the formation of complex/hybrid-type glycosylated NTB-A. Furthermore, this phenomenon is associated with the transport of NTB-A to the cell surface.

The second cytoplasmic alpha helix of Vpu and/or its localization in the Golgi-compartment appears to be critical to prevent the formation of the mature form of NTB-A. The importance of Vpu-mediated downmodulation of NTB-A is highlighted by our observation

that this function is conserved among diverse HIV-1 and SIV strains. One notable exception are the Vpu proteins derived from HIV-1 group N, which fail to affect the glycosylation pattern of NTB-A and do not induce downregulation of cell surface NTB-A. Altogether, our data suggest that Vpu influences the glycosylation pattern of NTB-A, which correlates with a decreased localization of NTB-A at the cell surface.

Results

HIV-1 Vpu modulates the glycosylation pattern of NTB-A, but not of tetherin

Recently, it was shown that HIV-1 Vpu downregulates cell surface NTB-A, thereby protecting HIV-1 infected cells from lysis by NK cells (Shah et al., 2010). At first, we evaluated a potential effect of Vpu on the protein turnover of NTB-A by *pulse-chase* experiments in 293T cells. In general, NTB-A is expressed in NK-, B- and T cells, and is not present on the surface of 293T cells (Valdez et al., 2004). 293T cells were cotransfected with an expression plasmid that is under control of the CMV promoter expressing NTB-A isoform 2 (pNTB-A-2) together with an expression plasmid for AU1-tagged pCG-HIV-1 M NL4-3 *wt* Vpu (pCG-HIV-1 M NL4-3 *wt* Vpu-AU1-IRES-GFP), or an empty vector control. 24 h post transfection cells were pulse labeled with [^{35}S]methionine and subjected to a chase period for up to 6 h. Cell lysates were immunoprecipitated with anti-NTB-A antibodies, separated by SDS-PAGE and analyzed by autoradiography (Fig. 1A). The NTB-A protein was initially synthesized as a single band with a molecular weight of approximately 50 kDa, which most likely represents the high mannose version of NTB-A (Fig.1A, upper left panel). After approximately 15 min of chase, a higher molecular version of NTB-A migrating at approximately 60 kDa starts to emerge, which most likely represents the complex/hybrid-type glycosylated form of NTB-A (Fig 1A, lower left panel). In contrast, the formation of the 60 kDa band of NTB-A was barely detectable in the presence of Vpu (Fig. 1A upper left panel). The quantification of the relative amount of the 50 kDa and 60 kDa version of NTB-A by phosphoimager analysis clearly demonstrates that Vpu prevents the formation of the mature form of NTB-A during the 6 h chase period (Fig. 1A, right panel). Similar results were obtained with NTB-A isoform 1 (pCG-NTB-A isoform 1) that contains an alanine insertion at amino acid position 266 (Fig. 1B).

Due to this observation we investigate whether other cellular targets of Vpu also share this phenomenon. Therefore, we analyzed whether Vpu affects the glycosylation pattern of tetherin. Tetherin contains two N-linked glycosylation sites at amino acid positions 65 and 92 (Kupzig et al., 2003) and was shown to become intensively glycosylated (Perez-Caballero et al., 2009). 293T cells were cotransfected with expression plasmids for Flag-tagged Tetherin (pCMV-Flag-Tetherin) and AU1-tagged *wt* Vpu or an empty vector control. 24 h post transfection cells were pulse labeled with [^{35}S]methionine and subjected to a *pulse-chase* protocol as conducted in Fig. 1A, B. In contrast to NTB-A, Vpu had no effect on the glycosylation pattern of tetherin (Fig. 1C, left side), while the stability of tetherin was slightly reduced in the presence of Vpu, which is consistent with previous reports (Douglas et al., 2009; Goffinet et al., 2010; Mangeat et al., 2009; Mitchell et al., 2009) (Fig. 1C, right panel). In contrast, the protein level of NTB-A remained stable, altogether indicating that Vpu's activity on NTB-A appears to be mechanistically distinct from the Vpu induced degradation of CD4 (Binette et al., 2007; Chen et al., 1993; Magadan et al., 2010; Willey et al., 1992) or the downregulation of cell surface tetherin (Neil, Zang, and Bieniasz, 2008; Shah et al., 2010; Van Damme et al., 2008).

NTB-A is not complexly glycosylated in the presence of Vpu

To study the effect of Vpu on the glycosylation pattern of NTB-A in more detail, we used Endoglycosidase H (Endo H) to remove high mannose oligosaccharides that are attached

during core glycosylation of newly synthesized proteins in the ER. Parallel cultures of 293T cells were cotransfected with pNTB-A-2 and AU1-tagged *wt* Vpu. *Pulse-chase* experiments were conducted as described in Fig. 1B. Half of the immunoprecipitated NTB-A was treated with Endo H, separated by SDS-PAGE, and analyzed by autoradiography. Similar to the results in Fig. 1, in the absence of Vpu the 50 kDa version of NTB-A was converted into the 60 kDa version within approximately 30 min of chase (Fig. 2B), a process that did not occur in the presence of Vpu (Fig. 2A, C left panel). Treatment with Endo H revealed that NTB-A remains completely Endo H sensitive throughout the chase period in the presence of Vpu, suggesting that Vpu most likely interferes with the transport of NTB-A through the secretory pathway (Fig. 2A, C right panel). In contrast, NTB-A became Endo H resistant in the absence of Vpu after approximately 30 min of chase, a time that is usually required for the formation of complex/hybrid-type glycosylated proteins in the secretory pathway (Fullekrug, Scheiffele, and Simons, 1999) (Fig. 2B, C right panel). In consistency with the results shown in Fig. 1, the 50 kDa as well as the completely deglycosylated version of NTB-A remain stable in the presence of Vpu. Thus, these results further support our notion that in contrast to tetherin and CD4, Vpu does not affect the half life of NTB-A, but rather affects its glycosylation pattern.

The Vpu-mediated changes in the glycosylation pattern of NTB-A correlate with a decreased localization of NTB-A at the cell surface

In order to analyze whether the Vpu induced downregulation of cell surface NTB-A correlates with the ability of Vpu to affect the glycosylation pattern of NTB-A, surface biotinylation analyses were performed. HeLa cells were transfected with pNTB-A-2 and an expression plasmid for AU1-tagged *wt* Vpu. 24 h post transfection cell surface proteins were biotinylated with Sulfo-NHS-LC-biotin. Cells were subsequently lysed and biotinylated proteins were immunoprecipitated with immobilized Streptavidin, separated by SDS-PAGE and analyzed by Western blot. NTB-A was recovered with Streptavidin, indicating that it was present at the cell surface in the absence of Vpu (Fig. 3A, lane 4), while in the presence of Vpu, the amount of cell surface NTB-A was significantly decreased (Fig. 3A, lane 6, C). Interestingly, the enrichment of cell membrane exposed NTB-A by Streptavidin pull-down reveals that the high mannose as well as the mature form of NTB-A localize at the cell surface (Fig. 3A, lane 6). This might indicate that Vpu does not affect NTB-A, once it has reached the plasma membrane (Fig 3A). The control protein, ribosomal P antigen 2 (RP2), which localizes exclusively in the cytoplasm, was not detectable after immunoprecipitation, while as another control the Transferrin receptor (TfR) localized at the cell surface (Fig. 3A). Consistent with the *pulse-chase* data, also in the steady state situation as measured by Western blot revealed that Vpu induces changes in the glycosylation pattern of NTB-A (Fig. 3B). Similar results were obtained in transfected 293T cells (data not shown). Thus, we could show that Vpu affects the glycosylation pattern of NTB-A (Fig. 3B), and that this phenomenon is associated with the ability of Vpu to inhibit the transport of newly synthesized NTB-A molecules to the cell surface.

Vpu delays the anterograde transport of newly synthesized NTB-A

Having provided biochemical evidence for reduced cell surface localization of NTB-A in the presence of Vpu, we next wanted to analyse the Vpu mediated effect on the transport of NTB-A to the cell surface by immunofluorescence in more detail. We adopted a microinjection approach, which was recently developed for the analysis of the anterograde transport of *de novo* expressed tetherin by confocal microscopy (Schmidt et al., 2011). To this end, expression plasmids were microinjected into the nuclei of TZM-bl cells and protein expression or localization was analysed at various time points post-injection. In the absence of Vpu, newly synthesized NTB-A was efficiently transported to the cell surface (over 25% and 80% of cells with detectable plasma membrane NTB-A at 2 h and 6 h post injection,

respectively (Fig. 4A)). Vpu significantly reduced such anterograde transport of newly synthesized NTB-A (only approximately 20% of cells with detectable plasma membrane NTB-A at 6 h post injection (Fig. 4A, NTB-A plasma membrane localization 6 h post injection in absence vs. presence of Vpu $p=\leq 0.05$)) and appeared to partially colocalize with NTB-A in a perinuclear compartment. This interference of NTB-A anterograde transport by Vpu represents a delay rather than a block of transport, since the plasma membrane localization of NTB-A continued to increase at later time points post injection (data not shown). These effects are distinct from the effect Vpu exerts on the anterograde transport of tetherin, where Vpu imposes a complete transport block that even remains stable over an extended period of time (Fig. 4B) (Dube et al., 2009; Schmidt et al., 2011). Moreover, Vpu-mediated trapping of tetherin in the TGN results in a concentration of tetherin in a defined subcellular compartment that persists over time. Similar colocalization in a defined perinuclear compartment was observed for NTB-A and Vpu 1 h post injection. At later time points Vpu did not entirely block the transport of NTB-A to the cell surface and the localization of NTB-A appeared to be more diffuse. In summary, these results suggest that Vpu slows down, but does not fully block, the anterograde transport of newly synthesized NTB-A.

Increased colocalization of NTB-A within the Golgi-compartment in presence of *wt* Vpu

Since Vpu affects glycosylation of NTB-A, we speculated that the anterograde transport of NTB-A is delayed at the level of the Golgi-apparatus. Therefore, we assessed colocalization of the galactosyltransferase-CFP fusion protein (GalT-CFP) (Rocks et al., 2010) and NTB-A in *wt* Vpu expressing HeLa cells in comparison to cells expressing only GFP or the truncated mutant Vpu Δ23, which does not contain α-helix 2 and is preferably expressed at the plasma membrane while its localization in the TGN is reduced (Dube et al., 2009; Pacyniak et al., 2005) (Fig. 5). Images were quantified by measuring the absolute percentage of pixels in the Golgi (GalT-CFP) that colocalize with NTB-A. Analyses of 195 cells revealed increased localization of NTB-A within the Golgi-compartment when *wt* Vpu was expressed (13.00%, n=80) in comparison to cells transfected only with GFP (6.936%, n=59) or the Vpu Δ23 mutant (9.550%, n=56) (Fig. 5). Importantly, the observed differences were statistically highly significant ($p<0.01$) in all cases. From these results we conclude that *wt* Vpu interferes with NTB-A trafficking by slowing down its passage through the Golgi-apparatus.

While the CK-2 phosphorylation sites are dispensable, the second α-helix of Vpu is critical to affect the glycosylation pattern and surface expression of NTB-A

To investigate the importance of the CK-2 phosphorylation sites and the second α-helix in the cytoplasmic domain for the Vpu-mediated effect on the glycosylation pattern and surface expression of NTB-A, a number of mutants were analyzed (Fig. 6A). 293T cells were cotransfected with either pNTB-A-2 and an expression plasmid for AU1-tagged *wt* Vpu, or mutants thereof. 24 h post transfection cells were lysed and the soluble protein fraction was analyzed by Western blot (Fig. 6B, D). The steady state situation reveals that the Vpu m26 mutant as well as the C-terminal deletion mutant Vpu Δ9, were capable of inducing the same changes in the glycosylation pattern of NTB-A as observed with *wt* Vpu (Fig. 6B). Furthermore, growing truncations of the second α-helix impeded Vpus ability to interfere with NTB-A glycosylation (Fig. 6D). The C-terminal deletion mutant Vpu Δ23 was strongly impaired in its activity on NTB-A glycosylation (Fig. 6B, D), indicating that this structural domain of Vpu might be imported for the effect on NTB-A. To further unravel the importance of the second α-helix in the cytoplasmic domain of Vpu to affect the glycosylation pattern of NTB-A, we investigated the Vpu Δ14 mutant, containing half of Vpu's second α-helix. This mutant has a decreased localization in the TGN similar to the Vpu Δ23 mutant (Dube et al., 2009). Interestingly, the Vpu Δ14 mutant had an intermediate

effect on the glycosylation pattern of NTB-A (Fig. 6D), further suggesting that the second α-helix in the cytoplasmic domain of Vpu is critical for Vpu's effect on NTB-A glycosylation. Moreover, the expression levels of all Vpu proteins were comparable (Fig. 6B, D).

In order to analyze whether the Vpu-mediated effect on the glycosylation pattern of NTB-A again correlates with a decreased surface expression of NTB-A, HeLa cells were cotransfected with either pNTB-A-2 and an expression plasmid for AU1-tagged *wt* Vpu, Vpu m26 or Vpu Δ23 along with GFP translated *via* an internal ribosomal entry site (Vpu-IRES-GFP) to monitor transfected cells. 24 h post transfection cells were harvested and stained for surface NTB-A, using a specific NTB-A antibody and analyzed by flow cytometry. The surface expression of NTB-A in Vpu positive cells was calculated as mean fluorescence intensity (MFI) of NTB-A expression in GFP positive cells, demonstrating that *wt* Vpu as well as Vpu m26 downregulate cell surface NTB-A (Fig. 6C). As expected, the Vpu Δ23 mutant only marginally downregulated cell surface NTB-A. Taken together, while the CK-2 phosphorylation sites of Vpu are dispensable, the second α-helix 2 in the cytoplasmic domain of Vpu seems to be required to affect the glycosylation pattern of NTB-A and to induce downregulation of cell surface NTB-A.

Vpu affects the glycosylation pattern and surface expression of NTB-A within post-ER compartments

To investigate whether localization of Vpu in the ER is required to affect the glycosylation pattern of NTB-A, *pulse-chase* analyses with the ER-trapped mutants Vpu A18H and Vpu-KKDQ were performed. It was previously shown that mutation of Ala-18 to His (A18H) results in an abnormal confinement of Vpu in the ER, similarly to the Vpu-KKDQ mutant that contains an ER retention signal at the C-terminus (Bolduan et al., 2011; Shikano and Li, 2003; Skasko et al., 2011; Vigan and Neil, 2011). Parallel cultures of 293T cells were cotransfected with pNTB-A-2 and expression plasmids for either *wt* Vpu, the Vpu Δ23-, Vpu A18H or the Vpu-KKDQ mutant. 24 h post transfection cells were pulse labeled with [^{35}S]methionine and chased for up to 2 h. After cell lysis, NTB-A molecules were immunoprecipitated with an anti-NTB-A antibody and the soluble protein fraction was analyzed by SDS-PAGE and autoradiography. As shown in Fig.7 A, only *wt Vpu* efficiently modulated the glycosylation pattern of NTB-A, while the mutants Vpu Δ23, Vpu A18H and Vpu-KKDQ exhibit an attenuated activity on NTB-A glycosylation (Fig. 7A), altogether indicating that ER confinement of Vpu abrogates its ability to affect the glycosylation pattern of NTB-A.

Next, we analyzed whether the Vpu mutants A18H or Δ23 are capable of inducing downregulation of endogenous cell surface NTB-A (Fig. 7B). Thus, primary CD4$^+$ T cells were infected with either the Vpu deletion mutant HIV-1 NL4-3 Vpu Del-1 and HIV-1 NL4-3 *wt,* HIV-1 NL4-3 Vpu A18H or HIV-1 NL4-3 Vpu Δ23, and surface expression of NTB-A was analyzed by flow cytometry. As expected, HIV-1 NL4-3 *wt* was capable of inducing downregulation of NTB-A from the cell surface (Fig. 7B). However, the Vpu deletion mutant HIV-1 NL4-3 Vpu Del-1 and the Vpu mutants HIV-1 NL4-3 Vpu A18H and HIV-1 NL4-3 Vpu Δ23 lost their ability to induce efficient downregulation of cell surface NTB-A (Fig. 7B). These results suggest that localization of Vpu within post-ER compartments is required to induce downregulation of NTB-A from the cell surface.

Confinement of NTB-A in the ER prevents the formation of complex/hybrid-type glycosylated NTB-A

Next, we investigated the effect of BFA on the glycosylation pattern of NTB-A by *pulse-chase* analyses. BFA is a fungal metabolite which blocks protein trafficking from the ER to

the Golgi complex and interrupts posttranslational processing occurring in the TGN (Misumi et al., 1986). Hence, parallel cultures of 293T cells were transfected with either, pNTB-A-2 together with an expression plasmid for AU1-tagged *wt* Vpu, or an empty vector control. 24 h post transfection half of the cells were incubated for 3 h with BFA or left untreated. Cells were pulse labeled with [^{35}S]methionine and chased for up to 2 h. After cell lysis, NTB-A was immunoprecipitated and analyzed by SDS-PAGE and autoradiography. In the absence of BFA and Vpu, the 50 kDa version of NTB-A was rapidly converted into the 60 kDa version within the standard, after approximately 30 min of chase. This conversion was completely abolished in the presence of BFA (Fig. 8), indicating that Vpu governs a mechanism that, at least in its outcome, is similar to the effect induced by BFA.

Tunicamycin and Glycopeptidase F (PNGaseF) completely deglycosylate NTB-A

We next analyzed the glycosylation pattern of NTB-A, using the N-linked glycosylation inhibitor Tunicamycin. Furthermore, we used PNGaseF, an enzyme that catalyzes the complete removal of N-linked oligosaccharide chains from glycoproteins (Norris et al., 1994). 293T cells were transfected with pNTB-A-2 and 4 h before cell lysis, cells were incubated with increasing amounts of Tunicamycin. Tunicamycin is a nucleoside antibiotic which inhibits N-linked glycosylation (Elbein, 1987; Tkacz and Lampen, 1975). Increasing concentrations of Tunicamycin induced the occurrence of a complete deglycosylated version of NTB-A and of a band with an apperent molecular weight of approximately 37 kDa (Fig. 9A). Furthermore, the glycosylation pattern of NTB-A was analyzed *via* PNGaseF digestion. To this end, 293T cells were transfected with pNTB-A-2 and an expression plasmid for *wt* Vpu or the Vpu Δ23 mutant and left untreated or treated with PNGaseF, respectively. 24 h post transfection the cells were lysed and subsequently treated with 500 U PNGaseF, separated by SDS-PAGE and analyzed by Western blot. In the absence of PNGaseF, *wt* Vpu was capable to induce changes in the glycosylation pattern of NTB-A (Fig. 9B). Consistently, this effect was not observed when the Vpu Δ23 mutant was expressed (Fig 9B), which was also confirmed by previous pulse chase data (Fig. 7A). After digestion with PNGaseF, only the deglycosylated form of NTB-A was detectable (Fig. 9B). As expected, no changes in the steady state protein level of NTB-A were observed (Fig. 9B). Thus, Vpu did not influence the stability of NTB-A, but selectively inhibited the formation of the complex/hybrid-type glycosylated NTB-A.

With the exception of HIV-1 group N, Vpu-mediated downmodulation of NTB-A is highly conserved among diverse primate lentiviruses

To examine to which extent the effect of Vpu on NTB-A is conserved among primate lentiviral Vpus, we analyzed the ability of various Vpu alleles of HIV-1 and SIV to affect the glycosylation pattern and surface expression of NTB-A. 293T cells were cotransfected with either pNTB-A-2 and expression plasmids for AU1-tagged Vpu derived from HIV-1 M NL4-3, SIV*gsn* 166, SIV*cpz* EK505, SIV*gor* CP2139 or HIV-1 N CK1.62. 24 h post transfection cells were lysed and analyzed by Western blot (Fig. 10A). The steady state situation revealed that Vpus derived from HIV-1 M NL4-3, SIV*gsn* 166, SIV*cpz* EK505, and SIV*gor* CP2139 are capable of inducing changes in the glycosylation pattern of NTB-A (Fig. 10A). Only Vpu derived from HIV-1 N lost its effect on NTB-A glycosylation. To investigate whether the Vpu-mediated effect on NTB-A glycosylation correlates with a decreased localization of NTB-A at the cell surface, HeLa cells were cotransfected with either pNTB-A-2 together with AU1-tagged Vpu derived from HIV-1 M NL4-3, SIV*gsn* 166, SIV*cpz* EK505, SIV*gor* CP2139 or HIV-1 N CK1.62. 24 h post transfection cells were harvested and stained for surface NTB-A, using a specific NTB-A antibody and analyzed by flow cytometry (Fig. 10B). In addition, cells were lysed, separated by SDS-PAGE and analyzed by Western blot, demonstrating that the expression levels of all Vpu proteins were comparable (Fig. 10B). Vpu proteins derived from HIV-1 M NL4-3, SIV*gsn* 166, SIV*cpz*

EK505, SIV*gor* CP2139 are capable of inducing downregulation of cell surface NTB-A. However, the Vpu protein derived from HIV-1 N lost its ability to induce efficient downregulation of cell surface NTB-A (Fig. 10B). This observation fits with the results obtained in Figure 10A. Thus, we conclude that the Vpu-mediated effect on NTB-A glycosylation is conserved among Vpu proteins of HIV-1 and SIV, and this phenomenon is associated with a decreased localization of NTB-A on the cell surface.

Discussion

In this study, we demonstrate that HIV-1 Vpu blocks the intracellular transport and thus the glycosylation pattern of the coactivating receptor NTB-A, which facilitates NK cell killing of virus infected cells (Bottino et al., 2001; Shah et al., 2010). This is particularly important, because HIV-1 Nef downregulates the inhibitory ligands HLA-A and –B, however not HLA-C and -E from the cell surface (Cohen et al., 1999). Further, another accessory protein HIV-1 Vpr upregulates the activating NKG2D ligands (ULBP-1, ULBP-2) (Ward et al., 2009), altogether increasing the susceptibility of HIV-1 infected cells for lysis by NK cells.

By *pulse-chase* kinetic analyses it was shown that Vpu prevents the formation of the complex/hybrid-type glycosylated version of NTB-A isoform 2 (Fig. 1A). Therefore, we speculated that Vpu interferes with the correct transport of NTB-A through the secretory pathway. Moreover, the glycosylation pattern of NTB-A isoform 1, which contains an alanine insertion at amino acid position 266, was also affected by Vpu similar to the NTB-A isoform 2 (Fig. 1B). Interestingly, the expression level of NTB-A isoform 1 (Ly108-1) in lymphocytes of lupus-prone mice is higher compared to that of NTB-A isoform 2 (Ly108-2), which correlated with an increased T cell antigen receptor-mediated calcium fluxes *in vitro* (Zhong and Veillette, 2008).

However, in contrast to NTB-A, Vpu has no effect on the glycosylation pattern of tetherin, but induces its degradation (Fig. 1C), suggesting that the effect of Vpu on the glycosylation pattern of NTB-A is mechanistically distinct from the Vpu induced downmodulation of tetherin.

In the absence of Vpu and upon treatment of NTB-A with Endo H, the mature form of NTB-A remains Endo H resistant after 30 min of chase (Fig. 2B), implying that the 60 kDa version of NTB-A most likely represents the complex/hybrid-type glycosylated version of NTB-A. In contrast, NTB-A remains Endo H sensitive (Fig. 2A) in the presence of Vpu, indicating that the 50 kDa version of NTB-A represents the high mannose form of NTB-A. However, it should be noted that Vpu does obviously not destabilize the deglycosylated or high mannose version of NTB-A, which is consistent with previous studies providing first evidence that Vpu does not alter the steady state protein level of NTB-A (Shah et al., 2010).

Next, it was investigated whether the Vpu-mediated effect on NTB-A glycosylation correlates with the ability of Vpu to downregulate NTB-A from the cell surface. In the presence of *wt* Vpu, a decreased localization of NTB-A at the cell surface was detectable (Fig. 3), indicating that Vpu interferes with the correct transport of NTB-A through the secretory pathway by disturbing its correct glycosylation.

Furthermore, a microinjection approach revealed that the anterograde transport of newly synthesized NTB-A is delayed in the presence of *wt* Vpu (Fig. 4A). This phenomenon fits with the observation that Vpu induces changes in the glycosylation pattern of NTB-A. Moreover, as control the anterograde transport of newly synthesized tetherin molecules is completely blocked in the presence of *wt* Vpu (Fig. 4B).

Indeed, quantitative colocalization analysis exploiting a Galactosyltransferase-CFP fusion protein as Golgi-marker (Rocks et al., 2010) revealed that NTB-A accumulated in the Golgi-apparatus in Vpu-expressing cells (Fig. 5). Consistent with the delayed, but not abrogated transport of NTB-A to the plasma membrane in the presence of Vpu, NTB-A was not completely retained in the Golgi complex. Furthermore, the Vpu Δ23 mutant showed an intermediate phenotype (Fig. 5), which fits well with the strongly reduced ability of this mutant to remove NTB-A from the cell surface (Fig. 6C). These results suggest that the post-ER interference of Vpu with NTB-A trafficking occurs at the site of the Golgi-apparatus, and therefore, represents a plausible mode of action how Vpu might block cell surface expression of cellular receptors.

In addition, we investigated whether CK-2 phosphorylation of Vpu is required to affect the glycosylation pattern of NTB-A (Fig. 6). The Vpu m26 mutant contains an exchange of two serine residues by asparagine at amino acid positions 52 and 56, which are essential to induce CD4 degradation by the ubiquitin-proteasome pathway (Binette et al., 2007; Magadan et al., 2010; Schubert et al., 1998). It was previously demonstrated that the Vpu m26 mutant is capable of inducing downregulation of NTB-A from the cell surface (Shah et al., 2010). In consistency, we show that the Vpu m26 mutant affected the glycosylation pattern and surface expression of NTB-A in a wild type manner (Fig. 6B, C), further supporting our notion that this phenomenon is mechanistically distinct from the Vpu induced inhibition of CD4 and tetherin (Schindler et al., 2010). However, the C-terminal deletion mutant Vpu Δ9, which was shown to have only marginal effects on the subcellular localization of the protein (Dube et al., 2009), also has no influence on the glycosylation pattern and surface expression of NTB-A (Fig. 6B, C), suggesting that the last 9 amino acids of Vpu's C-terminus are not involved in this mechanism. As shown previously, the Vpu Δ23 mutant, which does not contain helix 2, but still maintained the CK-2 phophorylation sites, has a significantly decreased localization in the TGN (Dube et al., 2009; Pacyniak et al., 2005). The Vpu Δ23 mutant was shown to be incapable to enhance virion release in the presence of tetherin (Dube et al., 2009) and to induce degradation of CD4 (data not shown). Interestingly, this mutant is attenuated in its ability to efficiently induce downregulation of cell surface NTB-A and to interfere with NTB-A glycosylation (Fig. 6B, C), indicating that the second α-helix and/or the localization of Vpu in the TGN are required for the Vpu-mediated effect on NTB-A. We could also demonstrate that the two ER-trapped mutants, Vpu A18H and Vpu-KKDQ, cannot affect the glycosylation pattern of NTB-A (Fig. 7A), furthermore supporting the notion that the effect of Vpu on NTB-A occurs within post-ER compartments.

Moreover, we show that the Vpu mutants HIV-1 NL4-3 A18H and HIV-1 NL4-3 Δ23 were strongly attenuated to induce downregulation of NTB-A in primary $CD4^+$ T cells (Fig. 7B), again indicating that localization of Vpu in post-ER compartments is required for the effect of Vpu on the glycosylation pattern and surface expression of NTB-A.

To investigate whether the Vpu-mediated effect on NTB-A glycosylation and the ability of Vpu to induce downregulation of cell surface NTB-A are conserved among primate lentiviral Vpus, we analyzed Vpu alleles from diverse HIV-1 and SIV strains (Fig. 10). Vpu proteins derived from HIV-1 M and its precursors SIV*gsn*, SIV*cpz* and SIV*gor* are capable of inducing changes in the glycosylation pattern of NTB-A (Fig. 10A). This phenomenon correlates with a decreased localization of NTB-A at the cell surface (Fig. 10B), indicating that the effect of Vpu on NTB-A is highly conserved among primate lentiviral Vpu proteins. However, Vpu derived from HIV-1 N has no influence on the glycosylation pattern of NTB-A and cannot induce efficient downregulation of cell surface NTB-A (Fig. 10A, B), suggesting that Vpu derived from HIV-1 N lost its anti-NTB-A activity.

In regard to the capacity of Vpu to retain glycoproteins in the exocytotic pathway, it was previously reported that Vpu is able to trap the HIV-1 glycoprotein gp120 and VSV-G in the ER/Golgi complex (Vincent and Abdul Jabbar, 1995). However, in contrast to the phenomenon we described herein, the authors reported that their effect requires the CK-2 phosphorylation of Vpu (Vincent and Abdul Jabbar, 1995). Currently, it is not clear whether our observation is specific for NTB-A or also applies for other host cell glycoproteins. Clearly, the effect of Vpu on viral glycoproteins (Vincent and Abdul Jabbar, 1995), which require the CK-2 phosphorylation, is part of a different mechanism that would be more related to Vpu's activity on CD4. Independent of this unresolved question, it is obvious that Vpu exerts different inhibitory activities within the secretory pathway (Dube et al., 2010; Matusali et al., 2012; Shah et al., 2010; Vincent and Abdul Jabbar, 1995).

Conclusion

Taken together, in this study we demonstrate that Vpu interferes with the anterograde transport of NTB-A at the site of the Golgi-compartment and induces changes in the glycosylation pattern of NTB-A by a post-ER mechanism. Moreover, with the exception of Vpu derived from HIV-1 group N, the Vpu-mediated effect on the glycosylation pattern and surface expression of NTB-A is conserved among lentiviral Vpu proteins of HIV-1 and SIV. This activity of Vpu might contribute to the detrimental effect of Vpu on other host cell factors.

Materials and Methods

Site-directed mutagenesis and plasmid constructions

All plasmids containing HIV-1 sequences are derivatives of the infectious molecular clone pNL4-3 (Adachi et al., 1986). The HIV-1 NL4-3 *wt* and HIV-1 Vpu Del-1 expression plasmids were described elsewere (Klimkait et al., 1990). Mutation of the HIV-1 NL4-3 Vpu A18H and HIV-1 NL4-3 Vpu Δ23 plasmids were introduced by site directed mutagenesis (Quick change Kit, Stratagene), using oligonucleotides, containing indicated changes. For cloning of the pCG-HIV-1 M NL4-3 Vpu Δ9-, pCG-HIV-1 M NL4-3 Vpu Δ23- and pCG-HIV-1 M NL4-3 Vpu-KKDQ-AU1-IRES-GFP mutants, the mutations were generated by PCR into the previously described pCG-IRES-GFP vector, expressing GFP from a bicistronic mRNA (Sauter et al., 2009; Schindler et al., 2003). The pCG-HIV-1 M NL4-3 *wt* Vpu-AU1-IRES-GFP, pCG-HIV-1 M NL4-3 Vpu A18H-AU1-IRES-GFP, pCG-HIV-1 M NL4-3 Vpu m26-IRES-GFP, pCG-nef STOP-IRES-GFP, pCG-SIV*gsn* 166 Vpu-AU1-IRES-GFP, pCG-SIV*cpz* EK505 Vpu-AU1-IRES-GFP, pCG-SIV*gor* CP2139 Vpu-AU1-IRES-GFP and pCG-HIV-1 N CK1.62 Vpu-AU1-IRES-GFP plasmids were described elsewhere (Bolduan et al., 2011; Sauter et al., 2009; Schindler et al., 2003). To generate the pcDNA3.3 TOPO-NTB-A isoform 2 (pNTB-A-2) expression plasmid, NTBA was amplified *via* PCR of the pCDONR223-SLAMF6 plasmid (addgene), using primers (NTB-A FOR: 5′ AAA CTC GAG ATG TTG TGG CTG TTC 3′ and NTB-A REV: 5′ AAA GGT ACC TCA CAA CAC GAC ATT 3′) and subcloned in the pcDNA3.3 TOPO plasmid, using the pCDNA™3.3-TOPO®TA Cloning® Kit (Invitrogen), leading to pcDNA3.3 TOPO-NTB-A isoform 2 (pNTB-A-2). NTB-A isoform 1 was amplified by PCR from pQCXIP-SLAM6, which was kindly provided by Edward Barker (Rush University Medical Center, Chicago). Restriction sites XbaI and MluI were added *via* the respective primers (NTB-A FOR: 5′ CGT CTA GAA TAT GTT GTG GCT GTT CCA ATC 3′ and NTB-A REV: 5′ CTA CGC GTT ACA CGA CAT TGT CAA GGG CAG 3′) and the PCR product was subcloned into the CMV promoter based expression vector pCG that directly expresses NTB-A isoform 1 together with GFP from a bicistronic mRNA (Schindler et al., 2003), using standard techniques. The pCMV-Flag-Tetherin, Vpu-GFP, pCFP-GalT and the HA-tagged tetherin

expression vector were described elsewhere (Banning et al., 2010; Bolduan et al., 2011; Rocks et al., 2010; Schmidt et al., 2011).

Cell culture

HeLa and 293T cells were cultivated in Dulbecco's modified Eagle medium (DMEM) supplemented with 10% heat inactivated fetal calf serum (FCS) and 2 mM L-glutamine, 100 U ml^{-1} penicillin and 100 mg ml^{-1} streptomycin.

$CD4^+$ T cells were maintained in RPMI 1640-FBS and were fed by replacing 80% of the medium at 2-day intervals. $CD4^+$ T cells were stimulated for 2 days with phytohemagglutinin [1μg/ml] and Interleukin-2 [100U/ml].

Western blot analysis

293T or HeLa cells were transiently transfected, using Lipofectamine 2000™ (Invitrogen) according to the manufacturer's protocol. 24 h post transfection, cells were lysed in 0.5% NP-40 lysis buffer (150 mM NaCl, 50 mM Tris-HCl, 0.5% Nonidet P-40 and a protease inhibitor cocktail (Roche)). Cell lysates were cleared by centrifugation at 10000 rpm and 4 °C for 5 min. NP-40 soluble proteins were separated in 12% SDS/PAA gels, according to Laemmli (Laemmli, 1970), transferred onto PVDF membranes (GE Healthcare) and probed with specific antibodies, followed by enhanced chemiluminescence detection. For internal controls, blots were stripped and re-incubated with the appropriate antibody.

Cell surface protein biotinylation

Cell surface proteins were biotinylated with EZ-Link Sulfo-NHS-LC-biotin (Thermo scientific) according to the manufacturer's protocol. Briefly, HeLa cells were washed three times with ice-cold phosphate-buffered saline (PBS), and primary amines of the membrane proteins exposed to the exterior of the cells were biotinylated with EZ-Link Sulfo-NHS-LC-biotin for 15 min at 4 °C. The cells were washed and lysed, using 0.5% NP-40 lysis buffer (150 mM NaCl, 50 mM Tris-HCl, 0.5% Nonidet P-40 and a protease inhibitor cocktail (Roche)). Biotinylated proteins were precipitated at 4 °C with immobilized Streptavidin (Thermo Scientific Pierce). Precipitated material was washed four times in 0.5% NP-40 buffer, separated in 12% SDS-PAA gel and analyzed by Western blot, using polyclonal anti-Vpu antiserum (rabbit) for detection of Vpu, anti-human NTB-A (BioLegend) for detection of NTB-A, human anti-ribosomal P antibody (Immunosion, INC) to detect ribosomal P antigen and mouse anti-Transferrin receptor (Invitrogen) to detect the Transferrin receptor. Data analysis was performed by using an Aida image analyzer (Raytest).

Metabolic labeling and immunoprecipitation

293T cells were cotransfected with either pNTB-A-2/pCG-NTB-A isoform 1 and pCG-HIV-1 M NL4-3 *wt* Vpu-AU1-IRES-GFP or Vpu mutants. 24 h post transfection, the cells were washed once with PBS (10 mM phosphate buffer [pH 7.4], 100 mM NaCl), and starved for 30 min in methionine- and cysteine-free RPMI 1640 medium (Sigma). Cells were pulse labeled with [^{35}S]methionine for 7 min at 37°C. The medium was then removed and equal aliquots were added to 1 ml of RPMI 1640-FBS for each time point of the chase period and incubated at 37°C. At the indicated time points, cells were collected and stored at −80°C. Cells were lysed, using 0.5% NP-40 lysis buffer. Immunoprecipitations were incubated for 3 h at 4°C, using GammaBind™ Plus Sepharose™ (GE Healthcare Bio-Science AB) coupled anti-NTB-A antibody (Bio Legend). Immunoprecipitated proteins were washed, using Triton wash buffer and solubilized by boiling in sample buffer containing 2% SDS, 1% 2-Mercaptoethanol, 1% glycerol, and 65 mM Tris hydrochloride (pH 6.8) and separated by SDS-PAGE. Gels were fixed for 120 min by incubation in 50% methanol, 10%

acetic acid and 20% glycerol, rinsed with water and dried. Radioactive bands were visualized by fluorography. Quantitation of the radioactivity of the bands was performed by using an Aida image analyzer.

In experiments involving BFA, cells were incubated for 3 h in RPMI 1640-FBS, supplemented with BFA [2 μg/ml], with a complete change of the medium after the first 2 h. Cells were then washed once in methionine- and cysteine-free RPMI 1640 medium (Sigma) containing 2 μg of BFA per ml and preincubated for 30 min in 5 ml of the same medium. Subsequently, cells were labeled for 7 min with [^{35}S]methionine (200 [μCi/ml]) and chased for up to 2 h. All steps were done in the presence of 2 μg of BFA per ml. During the chase period, fresh BFA [2 μg/ml] was added every 2 h. In experiments involving Endo H, cells were incubated for 30 min at 37°C in methionine and cysteine-free RPMI 1640 medium (Sigma), pulse labeled with [^{35}S]methionine for 7 min and chased for up to 2 h. After cell lysis, using 0.5% NP-40 lysis buffer, NTB-A molecules were immunoprecipitated for 3 h at 4°C, using GammaBind™ Plus Sepharose™ (GE Healthcare Bio-Science AB) coupled anti-NTB-A antibody (Bio Legend). Bead-bound material was split and either treated with 100 U Endo H (New England Biolabs) for 50 min at 37°C or left untreated. Samples were separated by SDS-PAGE and labeled proteins were visualized *via* autoradiography.

In experiments involving tetherin, 293T cells were cotransfected with either pCMV-Flag-Tetherin or pCG- *wt* Vpu-AU1-IRES-GFP. 24 h post transfection cells were incubated for 30 min at 37°C in methionine and cysteine-free RPMI 1640 medium (Sigma), pulse labeled with [^{35}S]methionine for 7 min at 37°C and chased for up to 2 h. After cell lysis, using RIPA buffer (50 mM Tris-HCl pH 7.4, 150 mM NaCl, 1% Nonidet P-40, 0.5% sodium deoxycholat, 0.1% Na-SDS, 5 mM EDTA, DNase, 1 mM PMSF and complete protease inhibitor cocktail (Roche)), tetherin molecules were immunoprecipitated for 3 h at 4°C, using anti-Flag M2 affinity matrix (Sigma). Samples were separated by SDS-PAGE and labeled proteins were visualized *via* autoradiography.

PNGaseF digestion

293T cells were cotransfected with either pNTB-A-2 and pCG-HIV-1 M NL4-3 *wt* Vpu-AU1-IRES-GFP or the pCG-HIV-1 M NL4-3 Vpu Δ23-IRES-GFP mutant. 24 h post transfection the cells were washed once with PBS and lysed, using 0.5% NP-40 lysis buffer. For glycopeptidase F digestion, cells were adjusted to 50 mM sodium phosphate [pH 7.5] and 1% NP-40, and incubated with 500 U of glycopeptidase F (New England Biolabs) for 30 min at 37°C. The digested samples were separated by SDS-PAGE and analyzed by Western blot, using polyclonal anti-Vpu antiserum (rabbit), anti-human NTB-A (BioLegend) and as loading control anti-β-actin (Sigma) antibodies. Data analysis was performed by using an Aida image analyzer (Raytest).

Tunicamycin treatment

293T cells were transfected with pNTB-A-2. Increasing amounts of Tunicamycin (50–500 ng/ml) were added to 1 ml of RPMI 1640-FBS 4 h before cell lysis. The cells were lysed, using 0.5% NP-40 lysis buffer, separated by SDS-PAGE and analyzed by Western blot, using polyclonal anti-Vpu antiserum (rabbit), anti-human NTB-A (BioLegend) and as loading control anti-β-actin (Sigma) antibodies.

HIV-1 infection of CD4$^+$ T cells

CD4$^+$ T cells were isolated from peripheral blood mononuclear cells (Buffy-Coat from the Institute for Transfusion Medicine in Suhl), which were prepared from gradient-isolated lymphocytes of a healthy HIV-seronegative individual, using human CD4-Micro-Beads (Miltenyi Biotec Inc.). For each infection, 5×10^6 CD4$^+$ T cells were stimulated for 2 days

with phytohemagglutinin [1 μg/ml] and Interleukin-2 [100U/ml]. The cells were infected with HIV-1 NL4-3 Vpu Del-1, HIV-1 NL4-3 *wt*, HIV-1 NL4-3 Vpu Δ23 and HIV-1 NL4-3 Vpu A18H. 7 days after infection, cells were analyzed by flow cytometry. $CD4^+$ T cells were maintained in RPMI 1640-FBS and were fed by replacing 80% of the medium at 2-day intervals. Virus stocks were prepared in 293T cells transfected with HIV-1 NL4-3 Vpu Del-1, HIV-1 NL4-3 *wt*, HIV-1 NL4-3 Vpu Δ23 and HIV-1 NL4-3 Vpu A18H plasmid DNA. Virus-containing supernatants were centrifuged at 1000 *g* for 5 min. Virions were purified by centrifugation through 20% sucrose at 20000 g for 90 min.

Flow cytometric analysis of Vpu-mediated downregulation of NTB-A

HeLa cells were cotransfected with either pNTB-A-2 and pCG-SIV*gsn* 166 Vpu-AU1-IRES-GFP, pCG-SIV*cpz* EK505 Vpu-AU1-IRES-GFP, pCG-SIV*gor* CP2139 Vpu-AU1-IRES-GFP, pCG-HIV-1 N CK1.62 Vpu-AU1-IRES-GFP, pCG- HIV-1 M NL4-3 *wt* Vpu-AU1-IRES-GFP or mutants. 24 h post transfection, the cells were harvested and stained for surface NTB-A, using an anti-NTB-A antibody (Bio Legend) and chicken anti-mouse Alexa647 conjugated secondary antibody (Molecular Probes, Invitrogen). NTB-A surface expression on GFP positive cells was then analyzed in a FACS LSRII, using FACSDiva software (BD Biosciences). Data analysis was performed by using FCS Express V3 software (De Novo).

$CD4^+$ T cells were infected with either HIV-1 NL4-3 Vpu Del-1, HIV-1 NL4-3 *wt* or HIV-1 NL4-3 Vpu A18H. 7 days after infection the cells were harvested and stained for surface NTB-A, using a NTB-A-specific antibody (BioLegend) and chicken anti-mouse Alexa647 conjugated secondary antibody (Molecular Probes, Invitrogen). Afterwards the cells were stained intracellularly for HIV-1 p24 antigen, using anti-KC57-FITC-specific antibody (COULTER CLONE®) and cell surface expression of NTB-A was analyzed in a FACS LSRII, using FACSDiva software (BD Biosciences). Data analysis was performed by using FCS Express V3 software (De Novo).

NTB-A anterograde biosynthetic transport assay

TZM-bl cells, grown on coverslips, were microinjected into their nuclei with an AIS 2 microinjection apparatus using pulled borosilicate glass capillaries in principle as previously reported (Schmidt et al., 2011). Plasmids encoding an HA-tagged tetherin that carries an HA epitope tag at position 154 in the extracellular domain (Tetherin-HA_{int}) or HA-tagged NTB-A and GFP or C-terminally GFP tagged Vpu, respectively, were mixed in H_2O at concentrations of 7 ng/μl and 10 ng/μl, respectively, and co-injected. Following microinjection, cells were cultured for 1, 2 or 6 hours at 37°C to allow protein expression and trafficking. At the indicated time points cells were fixed with 4% paraformaldehyde/PBS and Tetherin-HA_{int} or HA-NTB-A molecules were detected using a mouse anti-HA mAb (Santa-Cruz) followed by a goat anti-mouse Alexa568 secondary antibody (Invitrogen). Newly synthesized Vpu molecules were detected by fluorescence emission of GFP. Stained cells were imaged with a Zeiss LSM 510 confocal microscope.

Confocal microscopy

HeLa cells were seeded on coverslips and cotransfected with pNTB-A-2 and either pCG-HIV-1 M NL4-3 *wt* Vpu-AU1-IRES-GFP, pCG-HIV-1 M NL4-3 VpuΔ23-IRES-GFP and pCG-nef STOP-IRES-GFP. To visualize the Golgi apparatus, cells were additionally transfected with a pCFP-GalT expression plasmid which encodes for a galactosyltransferase fusion protein (Rocks et al., 2010). Immunofluorescence staining was essentially done as described previously (Koppensteiner et al., 2012). Briefly, 48 hours post transfection cells were once washed with PBS and fixed with 2% paraformaldehyde/PBS for 20 minutes at 4°C. Afterwards, cells were permeabilized with 1% Saponin/PBS for 15 min at RT,

followed by a blocking step using 5% BSA (Bovine serum albumin)/PBS for 45 min at RT. For immunostaining of NTB-A mouse anti-NTBA (Bio Legend) and goat anti-mouse Alexa555 conjugated secondary antibody (Invitrogen) was used. The coverslips were mounted on microscope slides using mowiol mounting solution (2.4 g polyvinylalcohol, 6 g Glycerin, 18 ml PBS) and imaged with a Zeiss LSM510 Meta. For colocalization studies, transfected cells were selected by GFP expression. Colocalization of NTB-A with the Golgi-compartment was analyzed by using Imaris (V6.4.2). Percentages of Golgi colocalizing with NTB-A were plotted and statistical analyzes were done using Graph Pad Prism (V5.0).

Acknowledgments

This work was supported by grants SFB643-A1, SFB796-A1, graduate program GRK1071, SCHU1125/3, SCHU1125/5-1, FA 378/11-1, SCHI1073/2-1 from the German Research Council, and the NIH grant RO1 DK81553. Furthermore, we acknowledge Addgene's distribution of the pDONR223 plasmid containing the SLAMF6 gene for non-commercial research use. We thank all members of the lab for discussions and critical study of this manuscript as well as Pia Rauch and Kirsten Fraedrich for their superior technical assistance.

References

Adachi A, Gendelman HE, Koenig S, Folks T, Willey R, Rabson A, Martin MA. Production of acquired immunodeficiency syndrome-associated retrovirus in human and nonhuman cells transfected with an infectious molecular clone. J Virol. 1986; 59(2):284–91. [PubMed: 3016298]

Banning C, Votteler J, Hoffmann D, Koppensteiner H, Warmer M, Reimer R, Kirchhoff F, Schubert U, Hauber J, Schindler M. A flow cytometry-based FRET assay to identify and analyse protein-protein interactions in living cells. PLoS One. 2010; 5(2):e9344. [PubMed: 20179761]

Binette J, Dube M, Mercier J, Halawani D, Latterich M, Cohen EA. Requirements for the selective degradation of CD4 receptor molecules by the human immunodeficiency virus type 1 Vpu protein in the endoplasmic reticulum. Retrovirology. 2007; 4:75. [PubMed: 17937819]

Bolduan S, Votteler J, Lodermeyer V, Greiner T, Koppensteiner H, Schindler M, Thiel G, Schubert U. Ion channel activity of HIV-1 Vpu is dispensable for counteraction of CD317. Virology. 2011; 416(1–2):75–85. [PubMed: 21601230]

Bottino C, Falco M, Parolini S, Marcenaro E, Augugliaro R, Sivori S, Landi E, Biassoni R, Notarangelo LD, Moretta L, Moretta A. NTB-A [correction of GNTB-A], a novel SH2D1A-associated surface molecule contributing to the inability of natural killer cells to kill Epstein-Barr virus-infected B cells in X-linked lymphoproliferative disease. J Exp Med. 2001; 194(3):235–46. [PubMed: 11489943]

Butticaz C, Michielin O, Wyniger J, Telenti A, Rothenberger S. Silencing of both beta-TrCP1 and HOS (beta-TrCP2) is required to suppress human immunodeficiency virus type 1 Vpu-mediated CD4 down-modulation. J Virol. 2007; 81(3):1502–5. [PubMed: 17121803]

Chen MY, Maldarelli F, Karczewski MK, Willey RL, Strebel K. Human immunodeficiency virus type 1 Vpu protein induces degradation of CD4 in vitro: the cytoplasmic domain of CD4 contributes to Vpu sensitivity. J Virol. 1993; 67(7):3877–84. [PubMed: 8510209]

Cohen EA, Terwilliger EF, Sodroski JG, Haseltine WA. Identification of a protein encoded by the vpu gene of HIV-1. Nature. 1988; 334(6182):532–4. [PubMed: 3043230]

Cohen GB, Gandhi RT, Davis DM, Mandelboim O, Chen BK, Strominger JL, Baltimore D. The selective downregulation of class I major histocompatibility complex proteins by HIV-1 protects HIV-infected cells from NK cells. Immunity. 1999; 10(6):661–71. [PubMed: 10403641]

Douglas JL, Viswanathan K, McCarroll MN, Gustin JK, Fruh K, Moses AV. Vpu directs the degradation of the human immunodeficiency virus restriction factor BST-2/Tetherin via a {beta}TrCP-dependent mechanism. J Virol. 2009; 83(16):7931–47. [PubMed: 19515779]

Dube M, Roy BB, Guiot-Guillain P, Binette J, Mercier J, Chiasson A, Cohen EA. Antagonism of tetherin restriction of HIV-1 release by Vpu involves binding and sequestration of the restriction factor in a perinuclear compartment. PLoS Pathog. 2010; 6(4):e1000856. [PubMed: 20386718]

Dube M, Roy BB, Guiot-Guillain P, Mercier J, Binette J, Leung G, Cohen EA. Suppression of Tetherin-restricting activity upon human immunodeficiency virus type 1 particle release correlates

with localization of Vpu in the trans-Golgi network. J Virol. 2009; 83(9):4574–90. [PubMed: 19244337]

Elbein AD. Glycosylation inhibitors for N-linked glycoproteins. Methods Enzymol. 1987; 138:661–709. [PubMed: 3600351]

Ewart GD, Sutherland T, Gage PW, Cox GB. The Vpu protein of human immunodeficiency virus type 1 forms cation-selective ion channels. J Virol. 1996; 70(10):7108–15. [PubMed: 8794357]

Flaig RM, Stark S, Watzl C. Cutting edge: NTB-A activates NK cells via homophilic interaction. J Immunol. 2004; 172(11):6524–7. [PubMed: 15153464]

Fullekrug J, Scheiffele P, Simons K. VIP36 localisation to the early secretory pathway. J Cell Sci. 1999; 112 (Pt 17):2813–21. [PubMed: 10444376]

Goffinet C, Homann S, Ambiel I, Tibroni N, Rupp D, Keppler OT, Fackler OT. Antagonism of CD317 restriction of human immunodeficiency virus type 1 (HIV-1) particle release and depletion of CD317 are separable activities of HIV-1 Vpu. J Virol. 2010; 84(8):4089–94. [PubMed: 20147395]

Iwabu Y, Fujita H, Kinomoto M, Kaneko K, Ishizaka Y, Tanaka Y, Sata T, Tokunaga K. HIV-1 accessory protein Vpu internalizes cell-surface BST-2/tetherin through transmembrane interactions leading to lysosomes. J Biol Chem. 2009; 284(50):35060–72. [PubMed: 19837671]

Klimkait T, Strebel K, Hoggan MD, Martin MA, Orenstein JM. The human immunodeficiency virus type 1-specific protein vpu is required for efficient virus maturation and release. J Virol. 1990; 64(2):621–9. [PubMed: 2404139]

Koppensteiner H, Banning C, Schneider C, Hohenberg H, Schindler M. Macrophage internal HIV-1 is protected from neutralizing antibodies. J Virol. 2012; 86(5):2826–36. [PubMed: 22205742]

Kuhl BD, Cheng V, Donahue DA, Sloan RD, Liang C, Wilkinson J, Wainberg MA. The HIV-1 Vpu viroporin inhibitor BIT225 does not affect Vpu-mediated tetherin antagonism. PLoS One. 2011; 6(11):e27660. [PubMed: 22110710]

Kupzig S, Korolchuk V, Rollason R, Sugden A, Wilde A, Banting G. Bst-2/HM1.24 is a raft-associated apical membrane protein with an unusual topology. Traffic. 2003; 4(10):694–709. [PubMed: 12956872]

Laemmli UK. Cleavage of structural proteins during the assembly of the head of bacteriophage T4. Nature. 1970; 227(5259):680–5. [PubMed: 5432063]

Magadan JG, Perez-Victoria FJ, Sougrat R, Ye Y, Strebel K, Bonifacino JS. Multilayered mechanism of CD4 downregulation by HIV-1 Vpu involving distinct ER retention and ERAD targeting steps. PLoS Pathog. 2010; 6(4):e1000869. [PubMed: 20442859]

Maldarelli F, Chen MY, Willey RL, Strebel K. Human immunodeficiency virus type 1 Vpu protein is an oligomeric type I integral membrane protein. J Virol. 1993; 67(8):5056–61. [PubMed: 8331740]

Mangeat B, Gers-Huber G, Lehmann M, Zufferey M, Luban J, Piguet V. HIV-1 Vpu neutralizes the antiviral factor Tetherin/BST-2 by binding it and directing its beta-TrCP2-dependent degradation. PLoS Pathog. 2009; 5(9):e1000574. [PubMed: 19730691]

Marassi FM, Ma C, Gratkowski H, Straus SK, Strebel K, Oblatt-Montal M, Montal M, Opella SJ. Correlation of the structural and functional domains in the membrane protein Vpu from HIV-1. Proc Natl Acad Sci U S A. 1999; 96(25):14336–41. [PubMed: 10588706]

Margottin F, Bour SP, Durand H, Selig L, Benichou S, Richard V, Thomas D, Strebel K, Benarous R. A novel human WD protein, h-beta TrCp, that interacts with HIV-1 Vpu connects CD4 to the ER degradation pathway through an F-box motif. Mol Cell. 1998; 1(4):565–74. [PubMed: 9660940]

Matusali G, Potesta M, Santoni A, Cerboni C, Doria M. The human immunodeficiency virus type 1 Nef and Vpu proteins downregulate the natural killer cell-activating ligand PVR. J Virol. 2012; 86(8):4496–504. [PubMed: 22301152]

Misumi Y, Miki K, Takatsuki A, Tamura G, Ikehara Y. Novel blockade by brefeldin A of intracellular transport of secretory proteins in cultured rat hepatocytes. J Biol Chem. 1986; 261(24):11398–403. [PubMed: 2426273]

Mitchell RS, Katsura C, Skasko MA, Fitzpatrick K, Lau D, Ruiz A, Stephens EB, Margottin-Goguet F, Benarous R, Guatelli JC. Vpu antagonizes BST-2-mediated restriction of HIV-1 release via beta-TrCP and endo-lysosomal trafficking. PLoS Pathog. 2009; 5(5):e1000450. [PubMed: 19478868]

Neil SJ, Zang T, Bieniasz PD. Tetherin inhibits retrovirus release and is antagonized by HIV-1 Vpu. Nature. 2008; 451(7177):425–30. [PubMed: 18200009]

Norris GE, Stillman TJ, Anderson BF, Baker EN. The three-dimensional structure of PNGase F, a glycosylasparaginase from Flavobacterium meningosepticum. Structure. 1994; 2(11):1049–59. [PubMed: 7881905]

Pacyniak E, Gomez ML, Gomez LM, Mulcahy ER, Jackson M, Hout DR, Wisdom BJ, Stephens EB. Identification of a region within the cytoplasmic domain of the subtype B Vpu protein of human immunodeficiency virus type 1 (HIV-1) that is responsible for retention in the golgi complex and its absence in the Vpu protein from a subtype C HIV-1. AIDS Res Hum Retroviruses. 2005; 21(5): 379–94. [PubMed: 15929700]

Perez-Caballero D, Zang T, Ebrahimi A, McNatt MW, Gregory DA, Johnson MC, Bieniasz PD. Tetherin inhibits HIV-1 release by directly tethering virions to cells. Cell. 2009; 139(3):499–511. [PubMed: 19879838]

Rocks O, Gerauer M, Vartak N, Koch S, Huang ZP, Pechlivanis M, Kuhlmann J, Brunsveld L, Chandra A, Ellinger B, Waldmann H, Bastiaens PI. The palmitoylation machinery is a spatially organizing system for peripheral membrane proteins. Cell. 2010; 141(3):458–71. [PubMed: 20416930]

Rong L, Zhang J, Lu J, Pan Q, Lorgeoux RP, Aloysius C, Guo F, Liu SL, Wainberg MA, Liang C. The transmembrane domain of BST-2 determines its sensitivity to down-modulation by human immunodeficiency virus type 1 Vpu. J Virol. 2009; 83(15):7536–46. [PubMed: 19474106]

Sauter D, Schindler M, Specht A, Landford WN, Munch J, Kim KA, Votteler J, Schubert U, Bibollet-Ruche F, Keele BF, Takehisa J, Ogando Y, Ochsenbauer C, Kappes JC, Ayouba A, Peeters M, Learn GH, Shaw G, Sharp PM, Bieniasz P, Hahn BH, Hatziioannou T, Kirchhoff F. Tetherin-driven adaptation of Vpu and Nef function and the evolution of pandemic and nonpandemic HIV-1 strains. Cell Host Microbe. 2009; 6(5):409–21. [PubMed: 19917496]

Schindler M, Rajan D, Banning C, Wimmer P, Koppensteiner H, Iwanski A, Specht A, Sauter D, Dobner T, Kirchhoff F. Vpu serine 52 dependent counteraction of tetherin is required for HIV-1 replication in macrophages, but not in ex vivo human lymphoid tissue. Retrovirology. 2010; 7:1. [PubMed: 20078884]

Schindler M, Wurfl S, Benaroch P, Greenough TC, Daniels R, Easterbrook P, Brenner M, Munch J, Kirchhoff F. Down-modulation of mature major histocompatibility complex class II and up-regulation of invariant chain cell surface expression are well-conserved functions of human and simian immunodeficiency virus nef alleles. J Virol. 2003; 77(19):10548–56. [PubMed: 12970439]

Schmidt S, Fritz JV, Bitzegeio J, Fackler OT, Keppler OT. HIV-1 Vpu blocks recycling and biosynthetic transport of the intrinsic immunity factor CD317/tetherin to overcome the virion release restriction. MBio. 2011; 2(3):e00036–11. [PubMed: 21610122]

Schubert U, Anton LC, Bacik I, Cox JH, Bour S, Bennink JR, Orlowski M, Strebel K, Yewdell JW. CD4 glycoprotein degradation induced by human immunodeficiency virus type 1 Vpu protein requires the function of proteasomes and the ubiquitin-conjugating pathway. J Virol. 1998; 72(3): 2280–8. [PubMed: 9499087]

Schubert U, Bour S, Ferrer-Montiel AV, Montal M, Maldarell F, Strebel K. The two biological activities of human immunodeficiency virus type 1 Vpu protein involve two separable structural domains. J Virol. 1996a; 70(2):809–19. [PubMed: 8551619]

Schubert U, Ferrer-Montiel AV, Oblatt-Montal M, Henklein P, Strebel K, Montal M. Identification of an ion channel activity of the Vpu transmembrane domain and its involvement in the regulation of virus release from HIV-1-infected cells. FEBS Lett. 1996b; 398(1):12–8. [PubMed: 8946945]

Schubert U, Henklein P, Boldyreff B, Wingender E, Strebel K, Porstmann T. The human immunodeficiency virus type 1 encoded Vpu protein is phosphorylated by casein kinase-2 (CK-2) at positions Ser52 and Ser56 within a predicted alpha-helix-turn-alpha-helix-motif. J Mol Biol. 1994; 236(1):16–25. [PubMed: 8107101]

Shah AH, Sowrirajan B, Davis ZB, Ward JP, Campbell EM, Planelles V, Barker E. Degranulation of natural killer cells following interaction with HIV-1-infected cells is hindered by downmodulation of NTB-A by Vpu. Cell Host Microbe. 2010; 8(5):397–409. [PubMed: 21075351]

Shikano S, Li M. Membrane receptor trafficking: evidence of proximal and distal zones conferred by two independent endoplasmic reticulum localization signals. Proc Natl Acad Sci U S A. 2003; 100(10):5783–8. [PubMed: 12724521]

Skasko M, Tokarev A, Chen CC, Fischer WB, Pillai SK, Guatelli J. BST-2 is rapidly down-regulated from the cell surface by the HIV-1 protein Vpu: evidence for a post-ER mechanism of Vpu-action. Virology. 2011; 411(1):65–77. [PubMed: 21237475]

Sowrirajan B, Barker E. The natural killer cell cytotoxic function is modulated by HIV-1 accessory proteins. Viruses. 2011; 3(7):1091–111. [PubMed: 21994772]

Strebel K, Klimkait T, Martin MA. A novel gene of HIV-1, vpu, and its 16-kilodalton product. Science. 1988; 241(4870):1221–3. [PubMed: 3261888]

Tkacz JS, Lampen O. Tunicamycin inhibition of polyisoprenyl N-acetylglucosaminyl pyrophosphate formation in calf-liver microsomes. Biochem Biophys Res Commun. 1975; 65(1):248–57. [PubMed: 167767]

Valdez PA, Wang H, Seshasayee D, van Lookeren Campagne M, Gurney A, Lee WP, Grewal IS. NTB-A, a new activating receptor in T cells that regulates autoimmune disease. J Biol Chem. 2004; 279(18):18662–9. [PubMed: 14988414]

Van Damme N, Goff D, Katsura C, Jorgenson RL, Mitchell R, Johnson MC, Stephens EB, Guatelli J. The interferon-induced protein BST-2 restricts HIV-1 release and is downregulated from the cell surface by the viral Vpu protein. Cell Host Microbe. 2008; 3(4):245–52. [PubMed: 18342597]

Vigan R, Neil SJ. Separable determinants of subcellular localization and interaction account for the inability of group O HIV-1 Vpu to counteract tetherin. J Virol. 2011; 85(19):9737–48. [PubMed: 21775465]

Vincent MJ, Abdul Jabbar M. The human immunodeficiency virus type 1 Vpu protein: a potential regulator of proteolysis and protein transport in the mammalian secretory pathway. Virology. 1995; 213(2):639–49. [PubMed: 7491787]

Ward J, Davis Z, DeHart J, Zimmerman E, Bosque A, Brunetta E, Mavilio D, Planelles V, Barker E. HIV-1 Vpr triggers natural killer cell-mediated lysis of infected cells through activation of the ATR-mediated DNA damage response. PLoS Pathog. 2009; 5(10):e1000613. [PubMed: 19798433]

Willey RL, Maldarelli F, Martin MA, Strebel K. Human immunodeficiency virus type 1 Vpu protein induces rapid degradation of CD4. J Virol. 1992; 66(12):7193–200. [PubMed: 1433512]

Zhong MC, Veillette A. Control of T lymphocyte signaling by Ly108, a signaling lymphocytic activation molecule family receptor implicated in autoimmunity. J Biol Chem. 2008; 283(28): 19255–64. [PubMed: 18482989]

Highlights

- HIV-1 Vpu induces downregulation of cell surface NTB-A to evade lysis of HIV-1 infected cells by NK cells.
- The effect on NTB-A is distinct from the Vpu-mediated downmodulation of CD4 and tetherin.
- Vpu prevents the formation of the complex glycosylated form of NTB-A by a post ER mechanism.
- Vpu affects the anterograde transport of newly synthesized NTB-A molecules at the site of the Golgi-apparatus.
- The effect of Vpu on NTB-A glycosylation is conserved among Vpu proteins of HIV-1 and SIV.

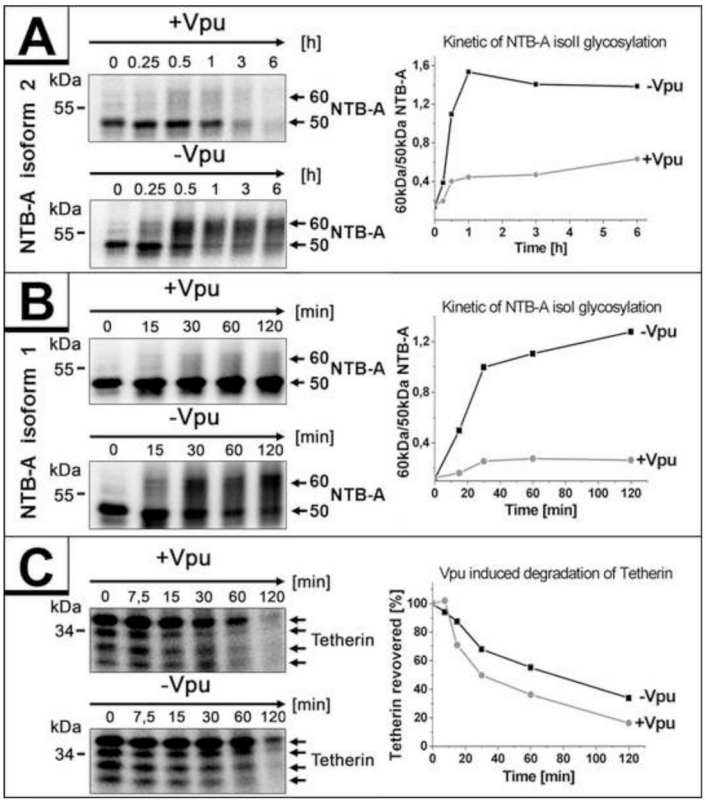

Figure 1. The effect of *wt* Vpu on the glycosylation pattern of NTB-A and tetherin analyzed *via pulse-chase* kinetic analysis

(A) Parallel cultures of 293T cells were cotransfected with pNTB-A-2 and either AU1-tagged *wt* Vpu or an empty vector control. 24 h post transfection cells were incubated in methionine free medium for 30 min and were then pulse labeled for 7 minutes with [^{35}S]-methionine. Cells were chased for up to 6 h and at each time point indicated cells were collected. NTB-A was immunoprecipitated with an anti-NTB-A antibody, analyzed by SDS-PAGE and autoradiography. Quantification of the kinetics of NTB-A isoform 2 glycosylation is given on the right. (B) Parallel cultures of 293T cells were cotransfected with NTB-A isoform 1 and either AU1-tagged *wt* Vpu or an empty vector control. 24 h post transfection cells were incubated in methionine free medium for 30 min and were then pulse labeled for 7 minutes with [^{35}S]-methionine. Cells were chased for up to 2 h, and at each time point indicated cells were collected. NTB-A was immunoprecipitated with an anti-NTB-A antibody, analyzed by SDS-PAGE and autoradiography. Quantification of the kinetics of NTB-A isoform 1 glycosylation is given on the right. (C) Parallel cultures of 293T cells were cotransfected with Flag-tagged tetherin and either AU1-tagged *wt* Vpu or an empty vector control. 24 h post transfection cells were incubated in methionine free medium for 30 min and were then pulse labeled for 7 minutes with [^{35}S]-methionine. Cells were chased for up to 2 h and at each time point indicated cells were collected. Flag-tagged tetherin was immunoprecipitated with anti-Flag M2 affinity matrix, analyzed by SDS-PAGE and autoradiography. Quantification of the Vpu induced degradation of tetherin is given on the right.

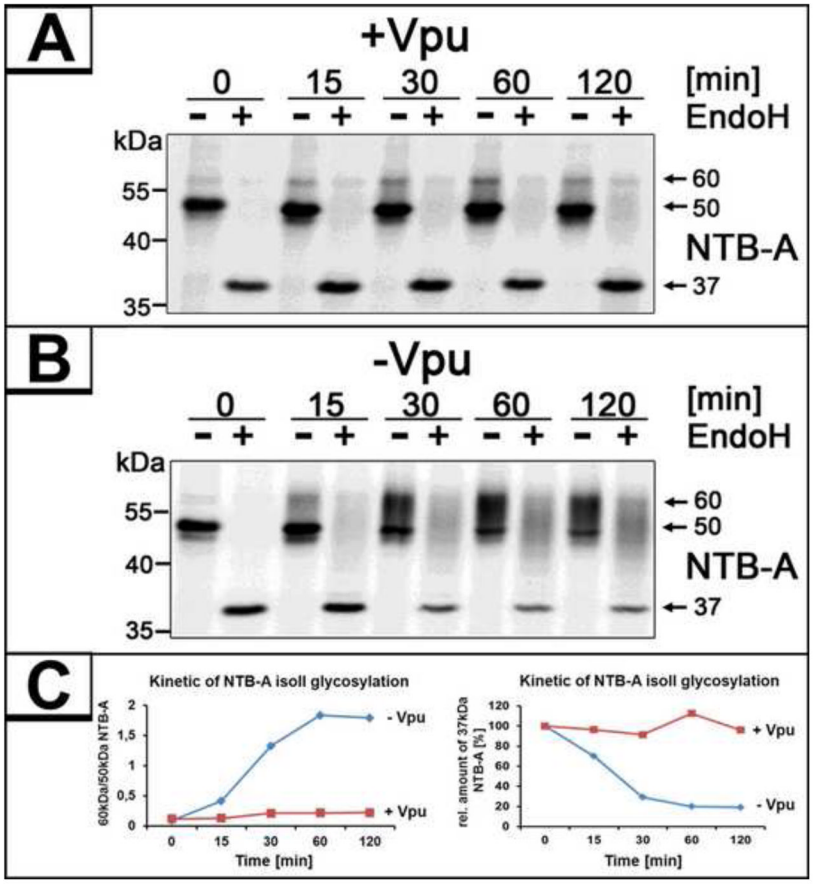

Figure 2. NTB-A remains Endo H sensitive in the presence of *wt* Vpu

Parallel cultures of 293T cells were cotransfected with either pNTB-A-2 alone (B) or together with AU1-tagged *wt* Vpu (A). 24 h post transfection cells were pulse labeled with [^{35}S]methionine for 7 min and chased for up to 2 h. NTB-A molecules were immunoprecipitated with an anti-NTB-A antibody. Bead-bound material was split and either treated with Endo H or left untreated. Samples were analyzed by SDS-PAGE and autoradiography. (C) Quantification of the kinetics of NTB-A isoform 2 glycosylation (the ratio of 60kDa/50kDa NTB-A is given on the left and the relative amount of 37kDa NTB-A is given on the right).

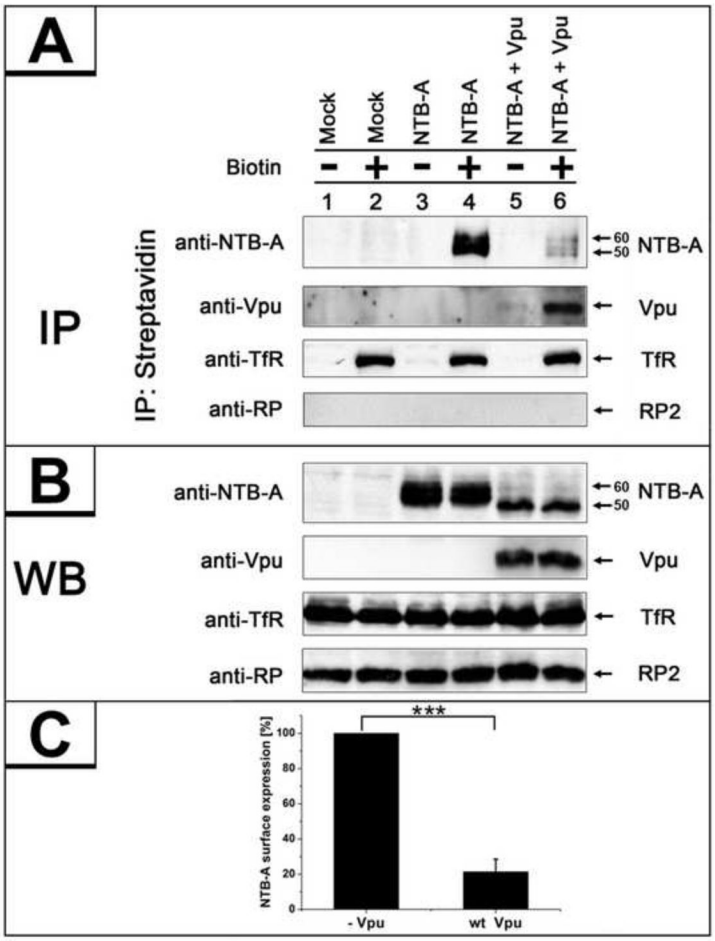

Figure 3. Cell surface biotinylation analysis of NTB-A in the presence or absence of *wt* Vpu

HeLa cells were cotransfected with either pNTB-A-2 or AU1-tagged *wt* Vpu. 24 h post transfection cell surface-expressed proteins were biotinylated. Upon cell lysis, biotinylated proteins were captured with immobilized streptavidin, separated by SDS-PAGE and analyzed by Western blot. NTB-A and *wt* Vpu were detected, using anti-NTB-A and polyclonal anti-Vpu antibodies. As positive control the Transferrin receptor and as negative control the ribosomal P antigen 2 were detected, using anti-Transferrin and anti-ribosomal P antigen antibodies. (A) Cell surface proteins after immunoprecipitation with Streptavidin. (B) Western blot control of whole cell lysates. (C) Quantification of relative NTB-A surface expression (*** $p \leq 0.05$, student's t-test). Bars represent mean ± SD from three independent experiments.

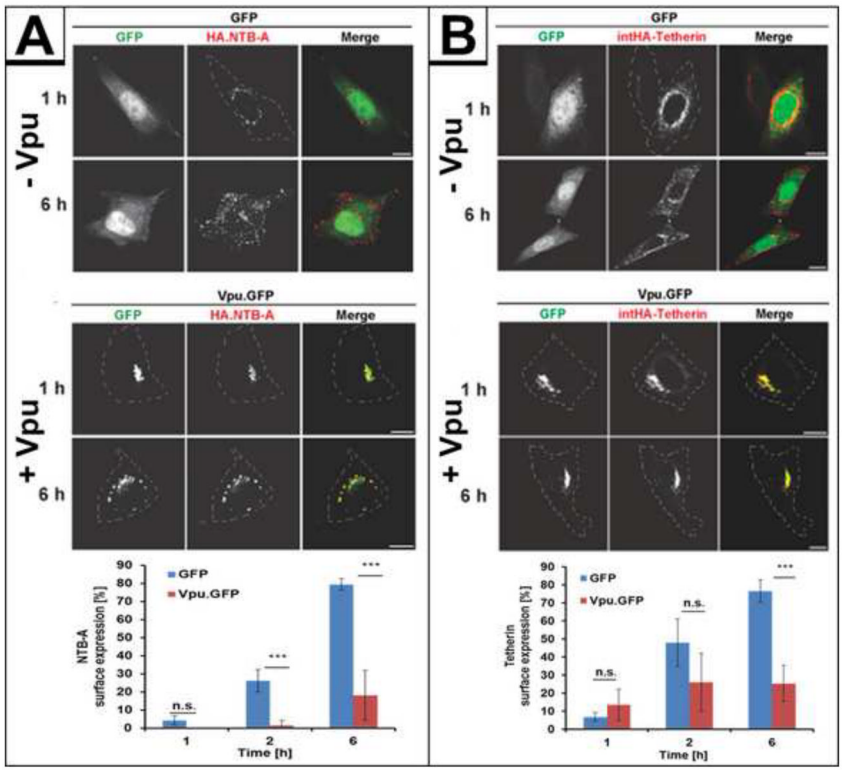

Figure 4. Vpu delays the anterograde transport of newly synthesized NTB-A to the cell surface

The nuclei of TZM-bl cells, grown on coverslips, were co-microinjected with expression plasmids for HA-tagged NTB-A (A) or Tetherin-HA ($_{int}$HA-Tetherin) (B) and vectors encoding GFP or Vpu.GFP. Subsequently, cells were cultivated for 1, 2, or 6 hours and then fixed, permeabilized and stained with an anti-HA mAb followed by an Alexa 568-conjugated secondary Ab (red staining) to detect newly synthesized HA-NTB-A or $_{int}$HA-Tetherin. Shown are representative microphotographs with indicated cell circumferences (upper panels). Scale bars: 10 μm. Cells were categorized into those with clear plasma membrane in addition to intracellular staining and cells with an exclusively intracellular staining of HA-NTB-A (A) or $_{int}$HA-Tetherin (B). Histogram bars (lower panels) depicting the relative percentage of cells with detectable plasma membrane staining for the indicated time points post microinjection. Shown are mean values with indicated standard deviation from three independent experiments with a total of at least 150 cells analyzed per plasmid combination (n.s. = non significant. ***; $p \leq 0.05$, student's t-test).

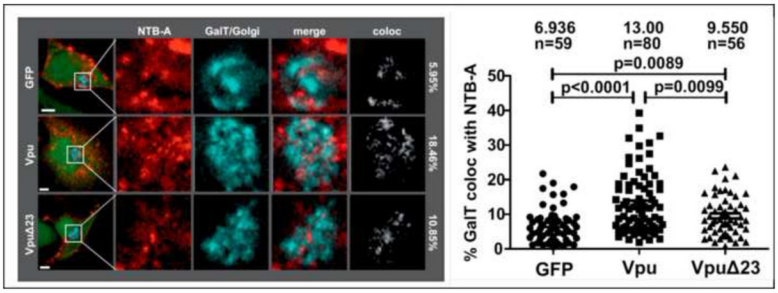

Figure 5. Colocalization of NTB-A within the Golgi-compartment

HeLa cells, grown on cover slips, were transfected with plasmids expressing GFP as a control, Vpu or Vpu Δ23 co-expressing GFP *via* an IRES element. Cells were cotransfected with NTB-A and the GalT-CFP fusion protein as a Golgi marker (blue). 48 hours later cells were fixed and NTB-A (shown in red) was stained by immunofluorescence. Transfected cells were identified by GFP expression and colocalization of Golgi (GalT-CFP) and NTB-A was quantified by the absolute percentage of GalT-CFP pixels which stain also positive for NTB-A using Bitplane Imaris V6.4.2 image analysis software. Values for a total of 195 analyzed cells were plotted and assessed for statistical significance by using the GrapPad Prism V5.0 software package. Scale bars: 5 μm.

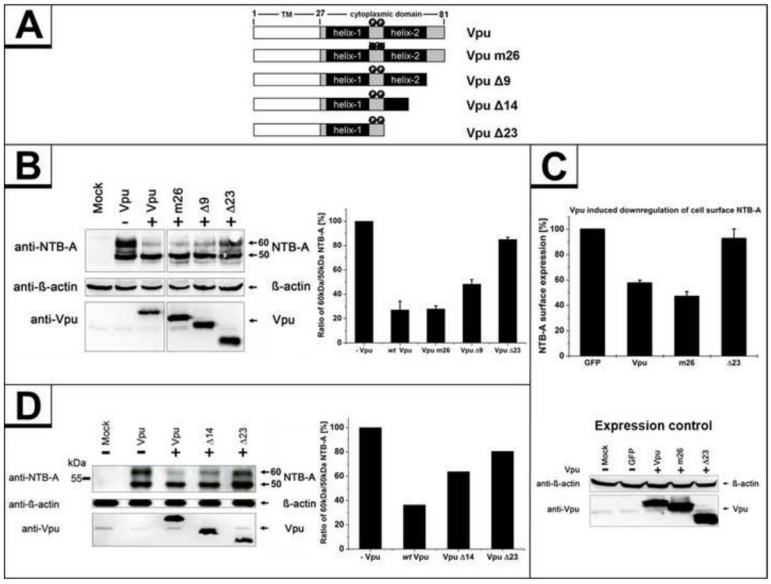

Figure 6. The ability of *wt* Vpu and Vpu mutants to affect the glycosylation pattern and surface expression of NTB-A

(A) Schematic representation of *wt* Vpu or the Vpu mutants m26-, Δ9-, Δ14- and Δ23. (B) 293T cells were cotransfected with either pNTB-A-2 and *wt* Vpu, m26, Δ9 or Δ23 mutant. 24 h post transfection cells were lysed and analyzed by Western blot, using anti-NTB-A, anti-Vpu and as loading control anti-β-actin antibodies. The ratio of 60kDa/50kDa NTB-A is given on the right. Bars represent mean ± SD from three independent experiments. (C) Summary of relative NTB-A surface expression. Bars represent mean ± SD from three independent experiments. HeLa cells were cotransfected with either pNTB-A-2 and AU1-tagged *wt* Vpu, Vpu m26 or Vpu Δ23. 24 h post transfection cells were harvested and stained for surface NTB-A, using a monoclonal NTB-A-specific antibody and analyzed by flow cytometry. In addition, cells were lysed and analyzed by Western blot, using anti-Vpu or anti-β-actin antibodies, which is given below. (D) 293T cells were cotransfected with either pNTB-A-2 and *wt* Vpu, Δ14 or Δ23 mutant. 24 h post transfection cells were lysed and analyzed by Western blot, using anti-NTB-A, anti-Vpu and as loading control anti-β-actin antibodies. The ratio of 60kDa/50kDa NTB-A is given on the right.

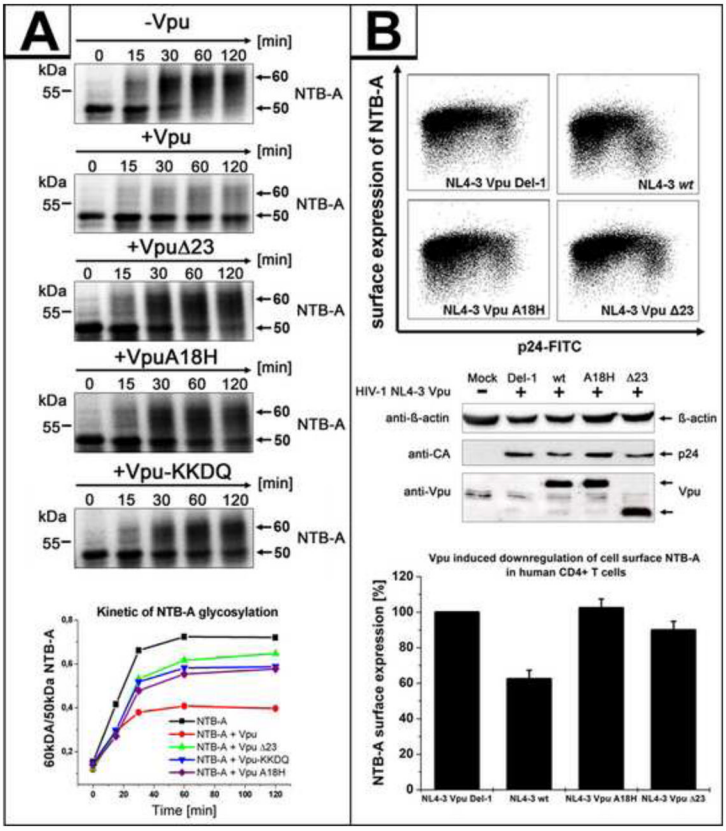

Figure 7. Confinement of Vpu in the ER abrogates its ability to affect the glycosylation pattern and surface expression of NTB-A

(A) Parallel cultures of 293T cells were cotransfected with either pNTB-A-2 alone or together with AU1-tagged *wt* Vpu, the Vpu Δ23 or the VpuA18H and Vpu-KKDQ mutants. 24 h post transfection cells were pulse labeled with [^{35}S]methionine for 7 min and chased for up to 2 h. NTB-A molecules were immunoprecipitated with an anti-NTB-A antibody, analyzed by SDS-PAGE and autoradiography. Quantification of the kinetics on NTB-A glycosylation is given below. (B) CD4^{+} T cells were infected with either HIV-1 NL4-3 Vpu Del-1, HIV-1 NL4-3 *wt*, HIV-1 NL4-3 Vpu A18H or HIV-1 NL4-3 Vpu Δ23 and 7 days after infection the cells were harvested and stained for surface NTB-A, using a NTB-A-specific antibody. Afterwards the cells were stained intracellularly for HIV-1 p24 antigen, using anti-p24-FITC specific antibody and analyzed by flow cytometry. In addition, cells were lysed and analyzed by Western blot, using anti-Vpu, anti-CA or anti-β-actin antibodies. Quantification of the relative surface expression of NTB-A is given below. Bars represent mean ± SD from three independent experiments.

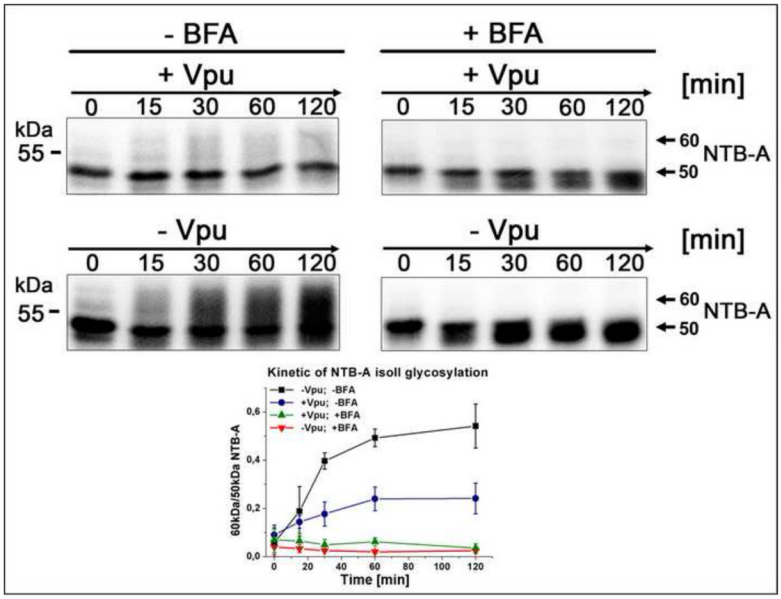

Figure 8. The effect of BFA on the glycosylation pattern of NTB-A

Parallel cultures of 293T cells were cotransfected with either pNTB-A-2 or AU1-tagged *wt* Vpu. 24 h post transfection half of each culture was incubated in RPMI 1640-FBS in the absence or presence of 2 μg of BFA per ml. Cells were then labeled for 7 min with [^{35}S]methionine, chased for up to 2 h, separated by SDS-PAGE and analyzed by autoradiography. All steps were performed in the presence of 2 μg of BFA per ml. Quantification of the kinetics of NTB-A isoform 2 glycosylation is given below. Bars represent mean ± SD from three independent experiments.

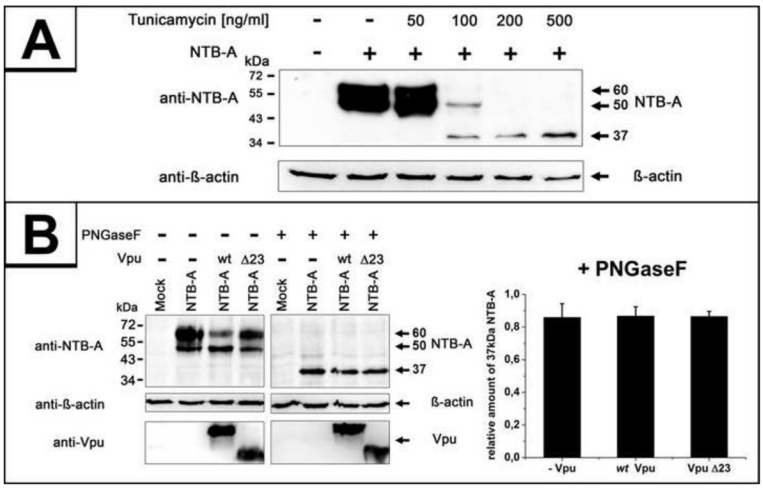

Figure 9. Analysis of the glycosylation pattern of NTB-A after treatment with Tunicamycin and PNGaseF

(A) Titration of Tunicamycin in the presence of NTB-A. 293T cells were transfected with pNTB-A-2 and 4 h before cell lysis, cells were treated with increasing amounts of Tunicamycin and analyzed by Western blot, using anti-NTB-A and as loading control anti-β-actin antibodies. (B) PNGaseF-digestion of NTB-A. 293T cells were cotransfected with either pNTB-A-2 and AU1-tagged *wt* Vpu or the Δ23 mutant, and then either treated with PNGaseF or left untreated. 24 h post transfection, the cells were lyzed and the soluble fraction was digested with PNGaseF and analyzed by Western blot, using anti-NTB-A-, anti-Vpu- and as loading control anti-β-actin antibodies. The relative amount of 37kDa NTB-A is given on the right. Bars represent mean ± SD from three independent experiments.

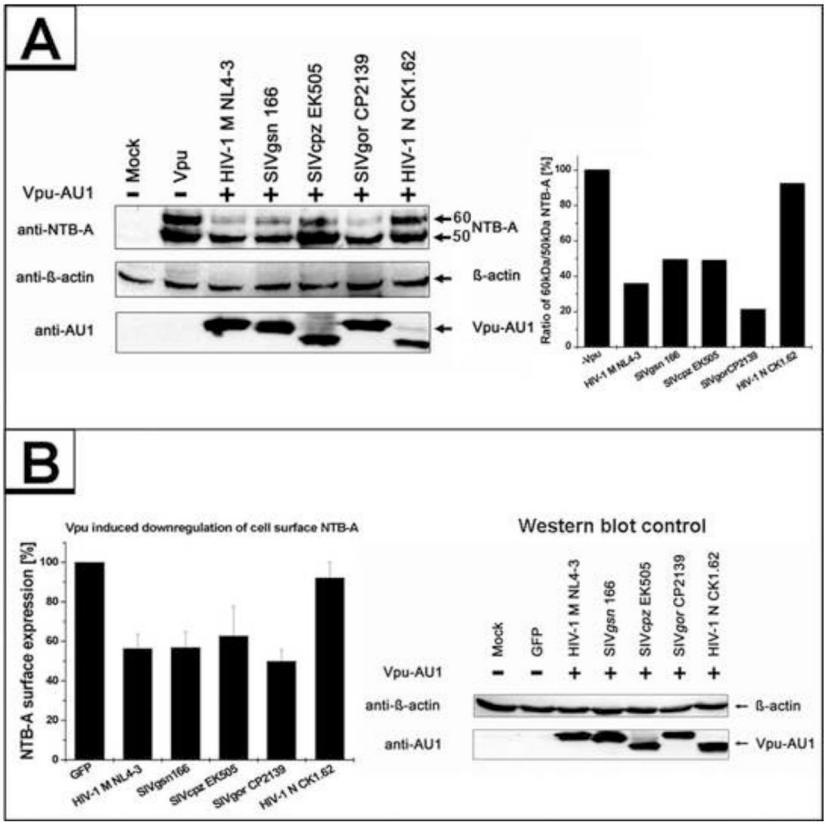

Figure 10. Effect of lentiviral Vpu proteins on the glycosylation pattern and cell surface expression of NTB-A

(A) 293T cells were cotransfected with either pNTB-A-2 and AU1-tagged Vpu of HIV-1 M NL4-3, SIV*gsn* 166, SIV*cpz* EK505, SIV*gor* CP2139 or HIV-1 N CK1.62. 24 h post transfection cells were lysed and analyzed by Western blot, using anti-NTB-A, anti-Vpu and as loading control anti-β-actin antibodies. The ratio of 60kDa/50kDa NTB-A is given on the right side. (B) HeLa cells were cotransfected with either pNTB-A-2 and AU1-tagged Vpu of HIV-1 M NL4-3, SIV*gsn* 166, SIV*cpz* EK505, SIV*gor* CP2139 or HIV-1 N CK1.62. 24 h post transfection cells were harvested and stained for surface NTB-A, using a monoclonal NTB-A-specific antibody and analyzed by flow cytometry. Summary of relative NTB-A surface expression is given on the left side. Bars represent mean ± SD from three independent experiments. In addition, cells were lysed and analyzed by Western blot, using anti-AU1 and anti-β-actin antibodies, which is given on the right side.